6-30-2017

Effect of Facial Encumbrance on Excimer Formation and Charge Resonance Stabilization in Model Bichromophoric Assemblies

Brandon Uhler
Marquette University

Maxim V. Ivanov
Marquette University

Damian Kokkin
Marquette University

Neil Reilly
Marquette University

Rajendra Rathore
Marquette University, rajendra.rathore@marquette.edu

See next page for additional authors

Accepted version. *The Journal of Physical Chemistry C*, Vol. 121, No. 29 (June 30, 2017): 15580-15588. DOI.

The Journal of Physical Chemistry C, Vol. 121, No. 29 (2017): 15580-15588. DOI.

Contents

Effect of Facial Encumbrance on Excimer Formation and Charge Resonance Stabilization in Model Bichromophoric Assemblies

Brandon Uhler
Department of Chemistry, Marquette University, Milwaukee, WI
Maxim V. Ivanov
Department of Chemistry, Marquette University, Milwaukee, WI
Damian Kokkin
Department of Chemistry, Marquette University, Milwaukee, WI
Rajendra Rathore
Department of Chemistry, Marquette University, Milwaukee, WI
Department of Chemistry, University of Massachusetts, Boston, MA
Scott A. Reid
Department of Chemistry, Marquette University, Milwaukee, WI

Abstract

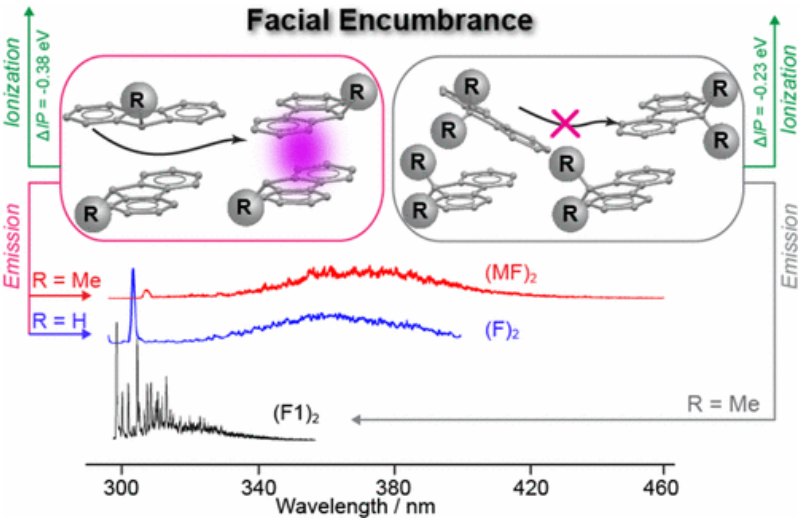

Excimer formation and charge resonance stabilization in covalently linked bichromophoric systems with flexible spacers are important processes relevant to biochemistry and functional materials. Requiring a π-stacked cofacial arrangement of a pair of aromatic molecules at a van

der Waals contact, the underlying geometrical reorganization that accompanies these events continues to be debated. Here we use a variety of methods including two-color resonant two-photon ionization spectroscopy (2CR2PI), ion yield measurements, hole-burning spectroscopy (HB), and laser-induced fluorescence (LIF) excitation and emission spectroscopy to compare the gas-phase spectroscopy and dynamics of the van der Waals dimers of fluorene, 9-methylfluorene (MF), and 9,9'-dimethylfluorene (F1). The goal of this work is to probe the influence of methyl substitution on the dynamics of excimer formation and charge resonance (CR) stabilization. The fluorene dimer, $(F)_2$, displays lifetime broadened electronic spectra and the dominance of excimer emission, consistent with a rapid (picoseconds) formation of a π-stacked excimer upon electronic excitation. Ion yield measurements of $(F)_2$ reveal a lowering of the ionization potential (IP) by some 0.38 eV relative to the monomer, reflecting significant CR stabilization. These trends are mirrored in the 9-methylfluorene dimer, $(MF)_2$, as one face of the π-system remains open. In contrast, the electronic spectrum of the dimethyl-substituted dimer, $(F1)_2$, shows narrow features representing a single band system, and analysis of the torsional structure in dispersed fluorescence spectra identifies this as emission from the locally excited state of a tilted (non-π-stacked) dimer, with no evidence of excimeric emission. The structure of this dimer reflects the increased importance of C–H/π interactions in the dimethyl-substituted system, as increased steric constraints block a cofacial approach. The IP of $(F1)_2$ shows CR stabilization which is roughly 1/2 of that in π-stacked $(F)_2$dimer. Extensive theoretical calculations support these findings and show the importance of sandwich-type configurations for excitonic delocalization and CR stabilization.

Introduction

Excimers (excited dimers) are bichromophores that are bound in the excited state but exhibit a repulsive interaction in the ground state.[1, 2] These simple systems serve as models for understanding excitonic interactions in multichromophoric systems, and the characteristic emission spectra of excimers and exciplexes (formed from two different chromophores) have been utilized in a variety of biological events and functional polymeric materials. Formation of excimers requires a π-stacked cofacial arrangement of a pair of aromatic molecules at a van der Waals contact, an arrangement which also leads to efficient charge stabilization.[3] However, the geometrical reorganization that accompanies these processes is not well understood, nor, indeed, is there a unified understanding of π-stacking interactions.[4]

Over the past two decades, van der Waals dimers of benzene and fluorene have been examined as model π-stacked systems.[5-8] The ground state structure of the benzene dimer has been extensively debated in the literature,[6, 7, 9-15] with recent high level *ab initio* studies confirming as the global minimum a tilted T-shaped structure stabilized by C–H/π interaction.[7, 14, 16] Upon excitation to the S_1 origin, only broad, red-shifted excimer emission is observed, indicating that the dimer undergoes rapid structural rearrangement in the excited state to a parallel sandwich excimer, the global minimum in the S_1 state, which has charge transfer character.[17] Calculations suggest that this rearrangement occurs over a small barrier, and thus the observation of excimer emission following excitation to the vibrationless level of S_1 has been attributed to tunneling, with a lifetime of several picoseconds inferred from the measured line widths.[17] While in the collisionless environment of a molecular beam the excited dimer

has no means to relax absent radiative decay, the much larger density of states in the excimer well presumably prevents back-tunneling.

Recently, Leutwyler and co-workers have re-examined the benzene dimer using two-color resonant two-photon ionization (2CR2PI) spectroscopy, supported with high level *ab initio* calculations.[16] This work has provided the first experimental identification of the S_2 state. Their calculations show that the oscillator strength for excimer emission is much smaller than resonant emission from T-shaped structures; indeed, resonant emission from the initially excited dimer state was observed upon excitation of the S_1 6_0^1 band.[17] Their calculations also provide a comprehensive view of the dimer to excimer transformation and confirm the hypothesis that the tilted T-shaped structure, while the global minimum in the ground state, is a local minimum in S_1.

As another model system, the fluorene dimer has also been extensively studied over the past two decades.[1-3, 8, 18-24] Here, electronic excitation also induces a rapid conversion to an excimer, evidenced in a broad, unstructured, and red-shifted emission band.[18-21] Using pump–probe fluorescence spectroscopy, Lim and co-workers showed that the primary decay pathway of the excimer is radiative.[1, 20, 21] These authors also mapped near-IR absorption from the excimer well using photodissociation spectroscopy.[20, 23] However, the geometrical reorganization from the locally excited dimer state to the excimer state has not been well characterized in this system, nor in fact is the structure(s) of the ground state dimer known, although a parallel displaced structure has often been assumed.[18-21]

Representing a significant advance in our ability to study π-stacked excimers, the Rathore group reported the synthesis and spectroscopic characterization of a novel set of polyfluorenes covalently linked at the 9-position through a single methylene spacer (these are denoted F*n*; *n* = 1–6).[25-28] These molecules adopt a cofacial arrangement in gas, liquid, and solid state and have been utilized as model systems to examine the energy and electron transport in π-stacked assemblies.[29] In a recent communication, we compared experimentally excimer stabilization (measured via emission) and charge stabilization (measured via threshold ionization) of covalently linked, cofacially stacked F2 with the van der Waals dimer of fluorene, i.e., $(F)_2$.[30] The measured ionization potentials were identical, yet the excimeric state was stabilized by up to ∼30 kJ/mol in covalently linked F2 (see structures in Scheme 1). Supported by theory, this work demonstrated that optimal stabilization of an excimer requires a perfect sandwich-like geometry with maximal overlap, whereas hole stabilization in π-stacked aggregates is less geometrically restrictive.

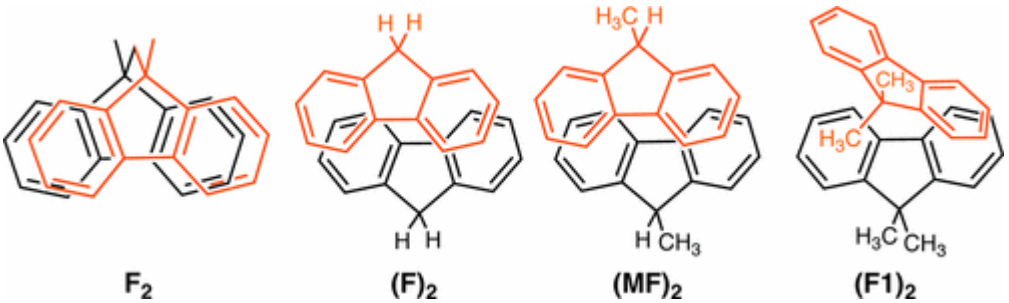

Scheme 1. Molecular Structures of Fluorene-Based Dimers Relevant to This Work

In this study, we compare the van der Waals dimers of fluorene (F), 9-methylfluorene (MF), and F1 (i.e., 9,9′-dimethylfluorene) to examine the influence of methyl substitution at the 9-position in fluorene on the efficiency of excimer formation and charge resonance (CR) stabilization. We expect the impact of a single methyl substitution to be small, as one face remains open for π-stacking, while double methyl substitution introduces additional steric constraints. Using a combination of gas-phase techniques including 2CR2PI, ion yield measurements, and laser-induced fluorescence (LIF) spectroscopy, supported by theory, our results allow a facile comparison of the relative stabilization of excimer vs hole (i.e., cation radical) in these model systems. In $(F)_2$ and $(MF)_2$, where calculations predict π-stacked minimum energy structures in S_0, the dimers evidence clear excimer formation and CR stabilization. However, for $(F1)_2$, excimer formation is quenched and CR stabilization is significantly reduced, as experiment and theory agree that the global minimum in S_0 corresponds to a tilted (non-π-stacked) structure, as dimethyl substitution at the 9-position prevents access to both π-surfaces of fluorene.

Methods

Experimental Methods

Resonant two-photon ionization (R2PI)[(31)] experiments were conducted in a linear 1 m time-of-flight mass spectrometer (TOFMS), equipped with a heated supersonic molecular beam source. A sample (typically 0.1–1%) of the species of interest in a rare gas (He or Ar) was generating by passing the gas through a heated solid sample cartridge which contained roughly 50 mg of the compound of interest trapped between loosely packed plugs of glass wool. The sample cartridge and nozzle, a solenoid-actuated pulsed valve (Parker-Hannifin), were heated up to temperatures of ∼250 °C using a flexible heater element; separate thermocouples were used to monitor temperature. The mixture was expanded at a total pressure of typically ∼1–2 bar from the 1.0 mm diameter nozzle, and the resulting gas pulse, of ∼1 ms duration, passed through a 1.0 mm diameter skimmer into the differentially pumped flight tube of a 1 m linear time-of-flight mass spectrometer. The flight tube vacuum was maintained by a 250 L/s turbomolecular pump, and a gate valve used to isolate the detector, which was kept under vacuum at all times. The main chamber was evacuated with a water-baffled diffusion pump (Varian VHS-4). With the nozzle on, typical pressures were $\sim 5 \times 10^{-5}$ mbar (main chamber) and $\sim 1 \times 10^{-6}$ mbar (flight tube). The background pressure in the flight tube could be lowered further by liquid nitrogen cooling of the vacuum shroud.

Several types of resonant ionization experiments were conducted. First, mass-selected excitation spectra were obtained using a one-color R2PI scheme (i.e., 1CR2PI), with laser light near 300 nm generated by frequency doubling in a BBO crystal the output of a dye laser (Lambda-Physik, Scanmate 2E), pumped by the second harmonic of a Nd:YAG laser (Continuum NY-61). Typical output pulse energies were 1–2 mJ in the doubled beam, which was loosely focused with a 1.0 or 2.0 m plano-convex lens into the chamber. Ions were extracted and accelerated using a conventional three-plate stack, with the repeller plate typically held at +2100 V, the extractor plate at +1950 V, and the third plate at ground potential. The ions traversed a path of 1 m prior to striking a dual chevron microchannel plate detector. The detector signal was amplified (×20) using a fast preamplifier (Femto HVA-500M-20B) and integrated using a boxcar system (Stanford Research SRS250) interfaced to a personal

computer. An in-house LABVIEW program controlled data acquisition and stepped the laser wavelength; typically, the signal from 20 laser shots was averaged per wavelength step.

Once the mass-selected excitation spectrum was obtained using 1CR2PI, a second frequency-doubled dye laser system (Sirah Cobra-Stretch pumped by second harmonic of Spectra-Physics INDI laser) was employed to perform two-color R2PI (i.e, 2CR2PI) experiments. Here, the timing of the two lasers was controlled using an eight-channel digital pulse/delay generator (Berkeley Nucleonics 565), and the conditions (focusing, energy, temporal and spatial overlap) were optimized to enhance the ratio of two-photon to one-photon signal. To determine ionization potentials, the excitation laser was tuned to the origin of the species of interest, and the ionization laser was scanned through the ionization threshold.

Hole-burning experiments were conducted to probe for the existence of multiple conformers. In these experiments, the third harmonic (355 nm) of a Continuum Minilite II Nd:YAG laser was used as the ionizing laser, and the INDI/Sirah system was employed as the hole-burning laser, the frequency of which was set to a specific feature in the spectrum of interest. Using the divide by *n*feature of the pulse generator, the Nd:YAG Q-switch of this laser was toggled at a repetition rate of 5 Hz, or a duty cycle 1/2 that of the nozzle and ionization laser(s), and the Q-switch delays was set so that the hole-burning laser preceded the ionizing (probe) laser(s) in time by 100–500 ns. The hole-burning spectrum was obtained using active subtraction on a shot-by-shot basis, where each shot obtained with only the ionizing (probe) laser(s) fired was subtracted from the preceding shot, where all lasers were fired. The subtracted signal was averaged over typically 20 laser shots and recorded as the probe laser was scanned.

Laser-induced fluorescence experiments were conducted in a separate chamber equipped with an identical molecular beam source, utilizing a mutually orthogonal geometry of laser, molecular beam, and detector, where the laser beam crossed the molecular beam at a distance of ∼15 mm (19 nozzle diameters) downstream. Here the timing of laser and nozzle firing was controlled by a four-channel digital pulse/delay generator (Berkeley Nucleonics model 575). The laser beam was not focused, and typical pulse energies were ∼0.5–1 mJ in an ∼3 mm diameter beam. Fluorescence was collected and collimated by a *f*/2.4 plano-convex lens and focused using a second 2 in. diameter *f*/3.0 lens either (a) through a long-pass cutoff filter onto a photomultiplier tube detector (PMT, Oriel 77348) for monitoring total fluorescence or (b) onto the slit of a 0.55 m monochromator/spectrograph (Horiba iHR550) equipped with a PMT detector (Oriel 77348) for dispersed fluorescence (DF) spectra. Fluorescence excitation spectra were acquired by integrating the PMT output using a gated integrator (Stanford Research SR250). The integrator output was digitized by a 12 bit ADC (Measurement Computing USB-1208FS) and passed to a computer for analysis. Typically, the signal was averaged over 20 laser shots at each wavelength step. Data collection and laser and monochromator control were achieved using LABVIEW software.

Computational Methods

To support our experimental findings, electronic structure calculations were performed using the GAUSSIAN 09 software package.[(32)] In an earlier benchmarking study of the benzene dimer,[(14)] we had found that accurate energies could be obtained using a simple PBE0 density

functional[33, 34] augmented with the D3 version of Grimme's dispersion term.[35] Thus, ground state calculations were performed at the PBE0-D3 level with def2-TZVP and/or def2-SV(P) basis sets.[36, 37] Optimizations employed an ultrafine Lebedev's grid with 99 radial shells per atom and 590 angular points in each shell; tight cutoffs were employed. Excited electronic states were computed using the time-dependent DFT. For the cation radical states, a calibrated[38-40] B1LYP40 functional with Grimme's dispersion term (B1LYP40-D3) was employed, with a 6-31G(d) basis set; wave function stability tests were performed to ensure the absence of states with lower energy (see Supporting Information for additional details).

Results and Discussion

Given the abundance of spectroscopic data for $(F)_2$ already available,[14, 15, 41] Figure 1 neatly summarizes the spectra recorded in this work in the region of the electronic origin using three different methods: LIF, 2CR2PI, and HB spectroscopy. As measured in different machines but under similar conditions with identical molecular beam sources, the LIF and 2CR2PI spectra are essentially identical. The origin spectrum is complex and has been analyzed in terms of two excitonic bands (i.e., S_1/S_2), split by some 20 cm^{-1},[41] with a progression in a single intermolecular mode giving rise to much of the substructure. The features display broadening consistent with lifetime broadening, and Lorentzian fits to features in the lower energy band indicate a homogeneous line width of 1.5 cm^{-1} (Figure S1 of the Supporting Information), suggesting that initial movement out of the Franck–Condon region occurs on a picoseconds time scale. The hole-burning spectrum obtained with the burn laser tuned to the lowest energy feature (arrowed, Figure 1) shows depletion of all features, indicating that only one conformer contributes to the spectrum. The likely identity of this conformer, elucidated with the aid of theory, is discussed below.

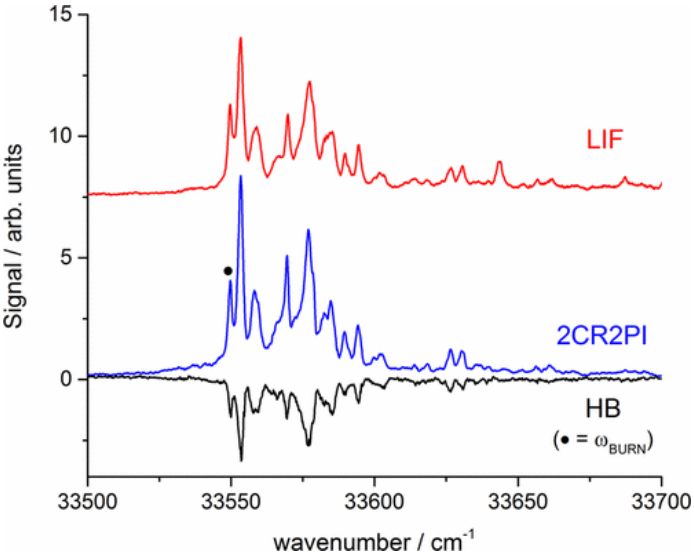

Figure 1. Laser-induced fluorescence (LIF), two-color resonant two-photon ionization (2CR2PI), and hole-burning (HB) spectroscopy of the fluorene dimer in the origin region. For the hole-burning spectrum, the burn laser was tuned to the lowest energy feature (marked).

In Figure 2, we show ion yield measurements for the fluorene monomer and van der Waals dimer, $(F)_2$, obtained in each case by tuning the excitation laser wavelength to the origin transition and scanning the ionization laser through threshold while monitoring ion signal at the mass of interest. The measured IP of the fluorene monomer is 7.885(1) eV, in agreement with, but more precisely determined than, the most recent literature value of 7.88(5) eV, obtained from ion/molecule equilibrium constant measurements.[42] In contrast, the measured IP of $(F)_2$ is 7.510(5) eV, lowered by 0.375 eV from the monomer. The dramatic reduction in IP reflects significant charge resonance stabilization in the dimer.

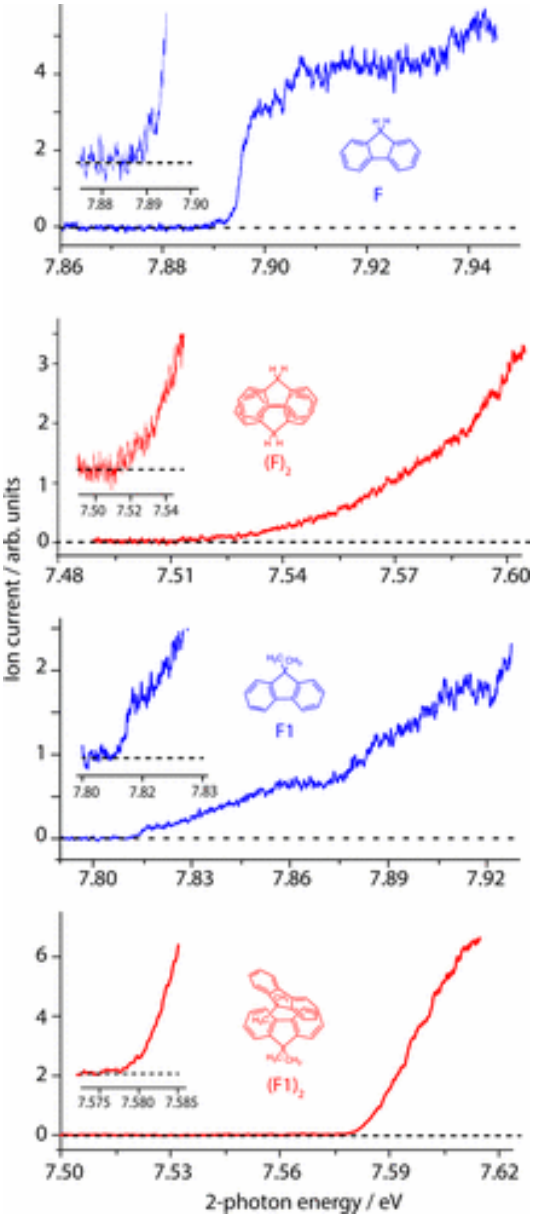

Figure 2. Ionization yield measurements of the fluorene dimer $(F)_2$, fluorene monomer,(30)$(F1)_2$ dimer, and F1 monomer (as indicated). Insets in each panel show expanded views of the region near ionization threshold.

Consistent with previous results,[18, 19] fluorescence measurements of $(F)_2$ reveal a lengthened fluorescence lifetime relative to the monomer (i.e., ~60 ns vs 15 ns), reflecting the nominally symmetry-forbidden transition. We observe no resolved emission features, only a very broad and unresolved band centered at 360 nm, as detailed below.[18, 19] The position of this band is in excellent agreement with that reported in fluorescence studies of concentrated fluorene solutions, where excimer emission was observed at a wavelength near 370 nm.[43]

Our data for $(F)_2$ are consistent with computational predictions of important stationary points on the ground and excited potential energy surfaces.[18, 19] Calculations identify two minima on the ground PES, corresponding to parallel orthogonal and parallel displaced π-stacked structures (Figure 3). The former lies 3.9 kJ/mol lower in energy and displays a rotation angle of ~94.5°. The observation of two excitonic components of similar intensity (Figure 1) is consistent with this structure, as the parallel-displaced structure would display one strong and one weak transition arising from the nearly parallel alignment of the transition dipoles. The observed excitonic splitting of $(F)_2$ is much smaller than the calculated static separation of ~130 cm^{-1}, which reflects vibrational quenching of the excitonic interaction, a phenomenon recently discussed by Leutwyler and co-workers.[44]

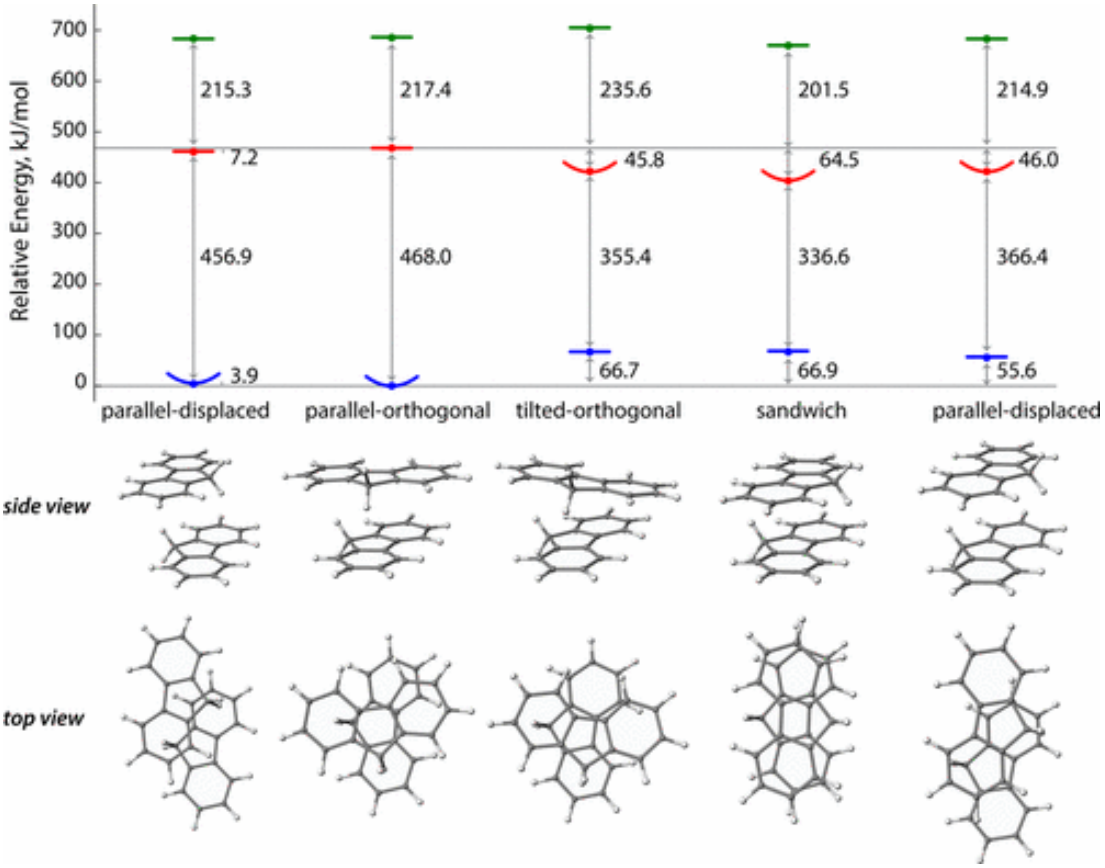

Figure 3. Calculated (B1LYP40-D3/6-31G(d)) stationary points of the fluorene dimer, $(F)_2$, in the ground (S_0), first excited (S_1), and ionized (D_0) state. Energies are given in kJ/mol. See Supporting Information for energies computed with the PBE0-D3/def2-SV(P) level of theory.

Following excitation of the $(F)_2$ S_1 origin, dispersed fluorescence (DF) spectra show only excimer-like emission, consistent with rapid (picoseconds) formation of an excimer.[18, 19] This conclusion is supported by calculations (Figure 3) which identify three distinct minima on the S_1 surface. The global minimum is a sandwich structure, lying 64.5 kJ/mol below the vertical S_1 energy of the parallel orthogonal structure. Calculations (Figures S2 and S3) predict that the sandwich structure produces maximal orbital overlap, and analysis of bond length changes in the electronic transition suggests that only in this structure the exciton is fully delocalized. As the excimer structure is a transition state on the ground PES, excimer emission is significantly red-shifted with respect to the excitation energy. The calculated energy gap (Figure 3, Tables S2 and S3) is in good agreement with the onset of emission observed experimentally.

In addition to the sandwich structure, two additional minima are predicted on the S_1 surface of $(F)_2$, corresponding to parallel displaced and tilted orthogonal structures (Figure 3). The latter is converted to the sandwich structure by passage over a barrier, calculated to lie roughly 12 kJ/mol below the vertical S_1 energy of the parallel orthogonal structure, and thus represents a plausible intermediate in the transformation. As in the collisionless environment of the molecular beam there is no mechanism to lose energy absent radiative decay, it is likely that all of these minima are sampled, in proportion to their density of states. The higher density of states in the excimer well(s) leads to the dominance of excimer emission. To summarize, then, from the ground state minimum of $(F)_2$, a parallel orthogonal geometry, electronic excitation leads to rapid (picoseconds) formation of an excimer, which is the global minimum on the excited PES(s). The sandwich structure is also the global minimum on the D_0 surface.

We next consider the van der Waals dimer of 9-methylfluorene (MF). Excitation spectra of $(MF)_2$obtained with 2CR2PI (Figure S4) are remarkably similar to those of $(F)_2$, both in appearance and in the red-shift from the respective monomer. This suggests a similar structure, both geometrically and electronically, for the two dimers. Indeed, the DF spectrum of $(MF)_2$ (Figure S5) shows only excimeric emission, with a lengthened fluorescence lifetime (25 ns, monomer; 100 ns, dimer). Our calculations of important stationary points on the ground and excited potential energy surfaces (Figure S6) also confirm that the single methyl substitution, which blocks a single π-face, has remarkably little effect on the dimer structure. We note that similar findings were evidenced by Itoh and Morita in studies of the 9-ethylfluorene (EF) dimer.[19]

Moving to the van der Waals dimer of 9,9'-dimethylfluorene (i.e, $(F1)_2$), the picture is expected to change dramatically, as the presence of an additional methyl group in F1 will eliminate, due to purely steric considerations, the possibility of forming a ground state structure in a parallel orthogonal geometry as well as sandwich-like structures on the S_1 and D_0 surfaces. Indeed, the excitation spectrum, as measured using 2CR2PI and shown in Figure 4, shows a set of sharp, narrow features only slightly red-shifted ($\sim$30 cm^{-1}) from the monomer origin. A hole burning spectrum (black curve in Figure 4) obtained with the burn laser tuned to the lowest energy transition shows depletion of all features, indicating the presence of a single conformer.

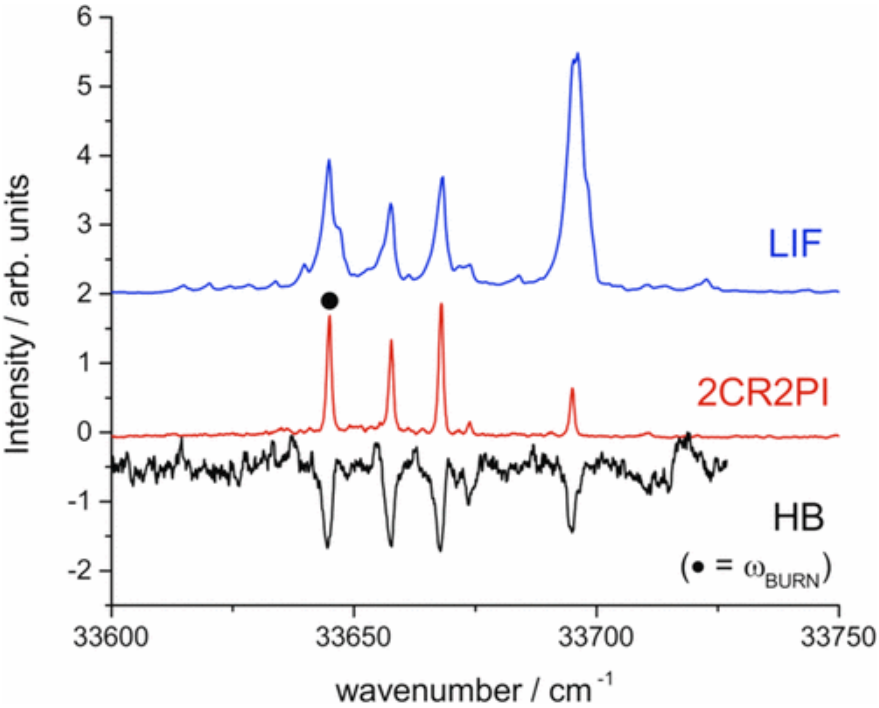

Figure 4. Spectrum of $(F1)_2$ obtained using LIF and 2CR2PI spectroscopy (above) and hole-burning spectroscopy (below). The most intense feature in the LIF spectrum is the origin band of the monomer. The HB spectrum shows depletion of all features and is consistent with the presence of a single conformer.

As another point of contrast, DF spectra of $(F1)_2$ obtained following excitation of the putative origin band show only structured emission (Figure 5), with no evidence of excimeric emission, confirmed by measuring DF spectra at different time delays. A high resolution DF (inset of Figure 5) of the low-frequency region shows well-resolved torsional structure, and additional torsional activity is observed upon excitation of the higher energy features in Figure 4. Table 1 presents the observed low-frequency transitions and their assignments, from which four fundamental torsional frequencies were obtained. Consistent with the lack of excimer emission, the measured fluorescence lifetime of $(F1)_2$, ca. 15 ns, is similar to that of the monomer.

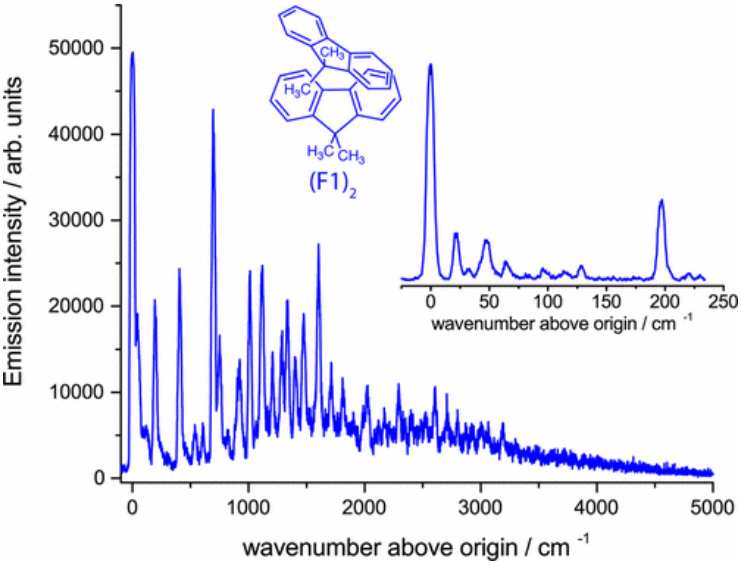

Figure 5. Dispersed fluorescence spectra of $(F1)_2$ obtained following excitation of the origin band (lowest energy feature in Figure 4). The inset shows a high resolution spectrum obtained with a 2400 lines/mm grating and reduced slit width, showing well-resolved torsional structure below 200 cm^{-1}.

Table 1. Experimental Vibrational Frequencies (in cm^{-1}) Derived from DF Spectra of $(F1)_2$ and Assignments

observed frequency	assignment	observed frequency	assignment
0		65	$2\omega_2$ or $3\omega_1$
22	ω_1	84	ω_4
33	ω_2	97	$2\omega_3$
44	$2\omega_1$	115	$2\omega_3 + \omega_1$
48	ω_3	129	$2\omega_3 + \omega_2$
56	$\omega_1 + \omega_2$		

Ion yield curves for the monomer and dimer of F1 are shown in Figure 2. Unlike the fluorene van der Waals dimer $(F)_2$, the yield curve of $(F1)_2$ displays an abrupt onset, indicative of a small geometry change between excited dimer and cation radical. The derived ionization potential of the dimer (7.577(1) eV) is 0.233 eV lower than that of the F1 monomer (7.810(1) eV), reflecting a significant CR stabilization, which, however, is roughly 40% smaller than found for the fluorene dimer.

As our technique allows the emission of a photon and ejection of electron to occur from the same structure, the absence of excimeric emission in $(F1)_2$ and reduced stabilization of the corresponding cation radical suggests that the structure of $(F1)_2$ dimer is vastly different than $(F)_2$or $(MF)_2$ in both ground and excited states. To aid in identifying the observed single conformer of $(F1)_2$, we turned to theory. Three distinct ground-state conformers (we label C1–C3 in energetic order) were optimized; these are shown (with relative energies in kJ/mol) in Figure 6. The global minimum structure (C1) and first local minimum (C2) are tilted (non-π-

stacked structures), where C–H/π interactions are important, while the highest energy structure (C3) here corresponds to a displaced π-stacked orientation. The calculated torsional frequencies of these conformers are compared in Table 2 with those derived from experiment. The two tilted conformers, C1 and C2, have frequencies most consistent with experiment.

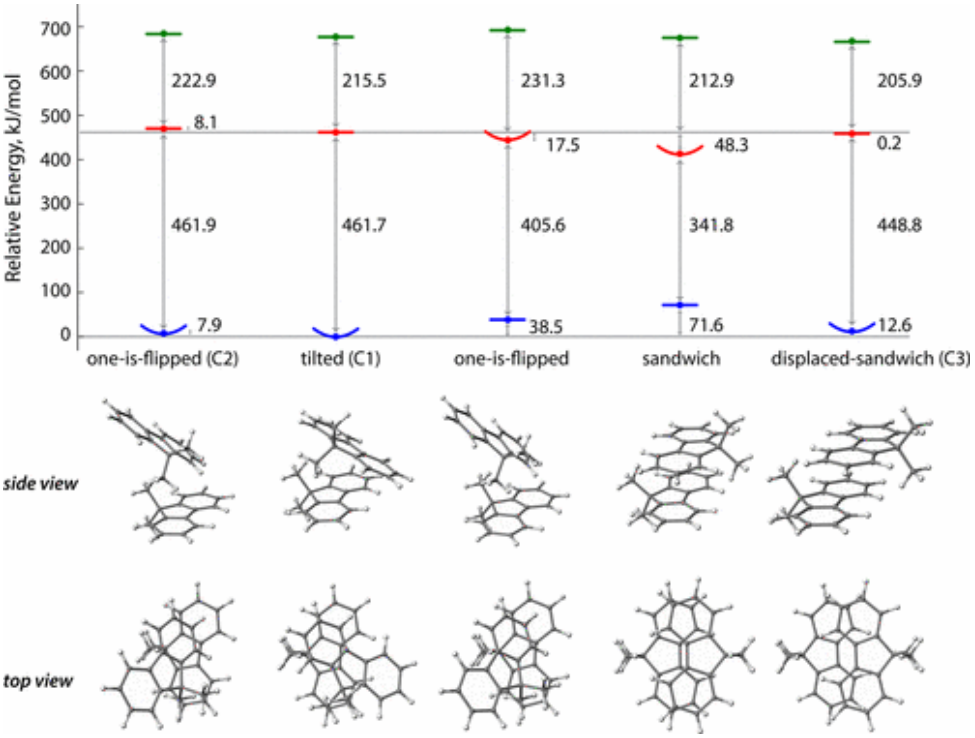

Figure 6. Calculated (B1LYP40-D3/6-31G(d)) stationary points of the 9,9′-dimethylfluorene dimer, $(F1)_2$, in the ground (S_0), first excited (S_1), and ionized (D_0) state. Energies are given in kJ/mol. See the Supporting Information for energies computed with the PBE0-D3/def2-SV(P) level of theory.

Table 2. Comparison of Torsional Harmonic Vibrational Frequencies of the $(F1)_2$Conformers C1–C3 Calculated at the PBE0-D3/Def2-SV(P) Level of Theory with Results from Experiment

mode	C1	C2	C3	expt
1	15.2	20.3	20.1	
2	22.4	22.0	26.2	22
3	33.0	35.8	41.6	33
4	53.6	53.0	50.7	48
5	58.9	61.0	62.9	
6	73.8	69.5	70.5	
7	94.1	89.4	81.5	84

The lack of evidence for excimer formation following excitation of the vibrationless level of $(F1)_2$may indicate a destabilization of the excimeric state due to steric interactions, the presence of a barrier to excimer formation in the S_1 state, or both. Theory finds a significant reduction in excimer well depth of $(F1)_2$ as compared with $(MF)_2$ or $(F)_2$ (compare Figures 3 and 6 with Figure S6). Starting from a tilted, non-π-stacked structure, it is plausible that a barrier to π-stacked excimer formation exists in the S_1 state. Unfortunately, it was not possible to test this assumption by examining via LIF higher excited vibrational levels in the S_1 manifold due to the strongly diagonal transition and overlap with bands of the monomer.

Finally, we note an important correspondence concerning the geometrical requirements for excimer formation as established in this work and charge-transfer (CT) complex formation of chloranil with hexamethylbenzene, hexaethylbenzene, and 1,3,5-trimethyl-2,4,6-triethylbenzene established in the work of Rathore et al.[45] shown pictorially in Figure 7. For hexamethylbenzene, where two π-faces are accessible, and 1,3,5-trimethyl-2,4,6-triethylbenzene, where one π-face is accessible, spontaneous association to form a CT complex is observed. However, complex formation is quenched in the case of hexaethylbenzene, where both π-faces are blocked. Similarly, in the case of 9,9-dimethylfluorene a pair of methyl groups hinder both faces of the fluorene moiety from attaining the excimer-like geometry, unlike fluorene and 9-methylfluorene (Figure 7).

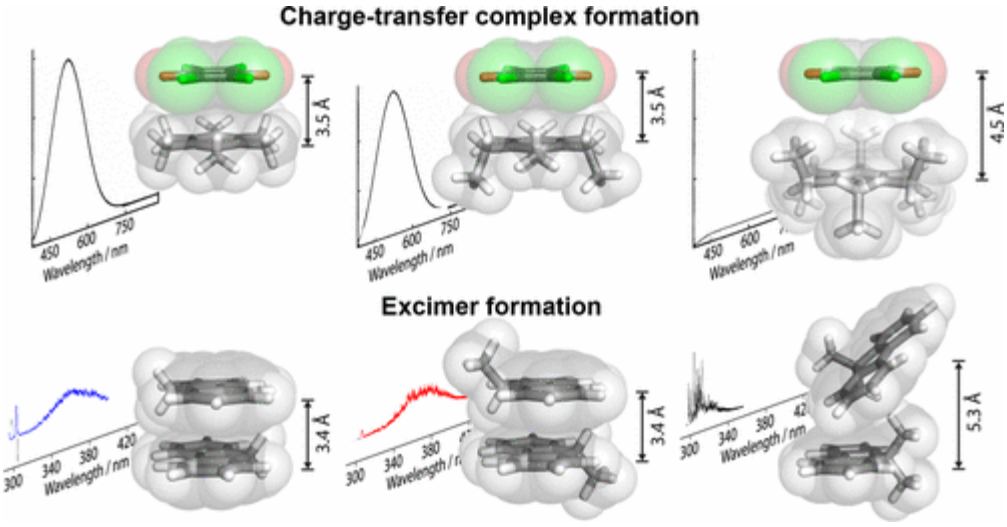

Figure 7. A comparison of the parallel effect of facial encumbrance in charge-transfer complex formation and excimer formation.

Conclusions

In this work, we have examined the energetics and dynamics of excimer formation and charge resonance stabilization in a set of model bichromophores consisting of the van der Waals dimers of jet-cooled fluorene (F), 9-methylfluorene (MF), and 9,9'-dimethylfluorene (F1). Hole-burning spectra suggest in each case the presence of a single conformer in the molecular beam; for the fluorene dimer $(F)_2$, this corresponds to an orthogonally π-stacked structure. Line widths

in the excitation spectra of $(F)_2$ suggest rapid (picoseconds) movement out of the Franck–Condon region on the excited surface, into the sandwich excimer well, which is the global minimum on the excited surface, as predicted by computational studies of the corresponding potential energy surfaces (PESs). Excimer formation is evidenced in broad, red-shifted emission and a lengthened fluorescence lifetime (relative to the monomer). Ion yield spectra indicate significant CR stabilization, as the sandwich structures are global minima in both S_1 and D_0 states.

These trends are mirrored in the spectra of $(MF)_2$, as single methyl substitution leaves accessible one π-face. In contrast, electronic spectra of the dimer obtained from the dimethyl derivative (i.e., $(F1)_2$) are very different, showing sharp structure and a much smaller red-shift relative to the monomer. Here, upon electronic excitation, only structured (nonexcimeric) emission is observed. Analysis of the low-frequency torsional structure in the DF spectra shows that the ground state minimum is a tilted (non-π-stacked) conformer, and it is likely that a barrier to excimer formation exists. Calculations predict a reduced stability of the excimeric state in comparison with $(F)_2$ and $(MF)_2$.

Charge resonance stabilization in the dimers was probed using ion yield spectroscopy (2CR2PI). Because of the rapid excimer formation upon excitation in $(F)_2$ (and $(MF)_2$), ionization occurs from the sandwich excimer structure, which calculations predict is the global minimum structure in both S_1 and D_0 states. In the case of $(F1)_2$, no excimer formation occurs and ionization proceeds from the tilted (non-π-stacked) ground state. While both $(F)_2$ and $(F1)_2$ display IPs reduced relative to the monomers, the relative CR stabilization is significantly larger in the π-stacked $(F)_2$ dimer. These findings underscore the differing geometrical requirements for excimer vs charge resonance stabilization in dimeric assemblies and the relative role of π-stacking and C–H/ π interactions in the stabilization of these clusters.

Supporting Information

The Supporting Information is available free of charge on the ACS Publications website at DOI: 10.1021/acs.jpcc.7b04255.

- Computational details, Figures S1–S6, and Tables S1–S7 (PDF)
- Equilibrium geometries of (F)2, (MF)2 and (F1)2 dimers optimized at neutral and first excited states (TXT)

Acknowledgment

Support by the National Science Foundation (Grant CHE-1508677) is acknowledged. We also thank Professor Marat R. Talipov for helpful discussions. The calculations were performed on the high-performance computing cluster Père at Marquette University funded by NSF Awards OCI-0923037 and CBET-0521602 and the Extreme Science and Engineering Discovery Environment (XSEDE) funded by NSF (TG-CHE130101).

References

Saigusa, H.; Lim, E. C. Excimer Formation in Van Der Waals Dimers and Clusters of Aromatic Molecules*Acc. Chem. Res.* **1996**, 29, 171– 178 DOI: 10.1021/ar950169v

Saigusa, H.; Lim, E. C. Excited-State Dynamics of Aromatic Clusters - Correlation between Exciton Interactions and Excimer Formation Dynamics *J. Phys. Chem.* **1995**, 99, 15738– 15747 DOI: 10.1021/j100043a010

Levy, D. H. Charge Transfer in Bichromophoric Molecules in the Gas Phase *Adv. Chem. Phys.* **1999**, 106,203– 220 DOI: 10.1002/9780470141656.ch4

Hunter, C. A.; Sanders, J. K. M. The Nature of π-π Interactions *J. Am. Chem. Soc.* **1990**, 112, 5525– 5534DOI: 10.1021/ja00170a016

Amicangelo, J. C. Theoretical Study of the Benzene Excimer Using Time-Dependent Density Functional Theory *J. Phys. Chem. A* **2005**, 109, 9174– 9182 DOI: 10.1021/jp053445o

Chipot, C.; Jaffe, R.; Maigret, B.; Pearlman, D. A.; Kollman, P. A. Benzene Dimer: A Good Model for π-π Interactions in Proteins? A Comparison between the Benzene and the Toluene Dimers in the Cas Phase and in an Aqueous Solution *J. Am. Chem. Soc.* **1996**, 118, 11217– 11224 DOI: 10.1021/ja961379l

Sinnokrot, M. O.; Sherrill, C. D. High-Accuracy Quantum Mechanical Studies of π-π Interactions in Benzene Dimers *J. Phys. Chem. A* **2006**, 110, 10656– 10668 DOI: 10.1021/jp0610416

Yip, W. T.; Levy, D. H. Excimer/Exciplex Formation in Van Der Waals Dimers of Aromatic Molecules *J. Phys. Chem.* **1996**, 100, 11539– 11545 DOI: 10.1021/jp9537668

Chandrasekaran, V.; Biennier, L.; Arunan, E.; Talbi, D.; Georges, R. Direct Infrared Absorption Spectroscopy of Benzene Dimer *J. Phys. Chem. A* **2011**, 115, 11263– 11268 DOI: 10.1021/jp204628g

Arunan, E.; Gutowsky, H. S. The Rotational Spectrum, Structure and Dynamics of a Benzene Dimer *J. Chem. Phys.* **1993**, 98, 4294– 4296 DOI: 10.1063/1.465035

Diri, K.; Krylov, A. I. Electronic States of the Benzene Dimer: A Simple Case of Complexity *J. Phys. Chem. A* **2012**, 116, 653– 662 DOI: 10.1021/jp209190e

Hobza, P.; Selzle, H. L.; Schlag, E. W. Structure and Properties of Benzene-Containing Molecular Clusters - Nonempirical Ab-Initio Calculations and Experiments *Chem. Rev.* **1994**, 94, 1767– 1785 DOI: 10.1021/cr00031a002

Law, K. S.; Schauer, M.; Bernstein, E. R. Dimers of Aromatic-Molecules - (Benzene)2, (Toluene)2, and Benzene Toluene *J. Chem. Phys.* **1984**, 81, 4871– 4882 DOI: 10.1063/1.447514

Sinnokrot, M. O.; Sherrill, C. D. Highly Accurate Coupled Cluster Potential Energy Curves for the Benzene Dimer: Sandwich, T-Shaped, and Parallel-Displaced Configurations *J. Phys. Chem. A* **2004**, 108, 10200–10207 DOI: 10.1021/jp0469517

Tsuzuki, S.; Uchimaru, T.; Sugawara, K.; Mikami, M. Energy Profile of the Interconversion Path between T-Shape and Slipped-Parallel Benzene Dimers *J. Chem. Phys.* **2002**, 117, 11216– 11221 DOI: 10.1063/1.1523057

Balmer, F. A.; Trachsel, M. A.; van der Avoird, A.; Leutwyler, S. The Elusive S-2 State, the S-1/S-2 Splitting, and the Excimer States of the Benzene Dimer *J. Chem. Phys.* **2015**, 142, 234306 DOI: 10.1063/1.4922608

Hirata, T.; Ikeda, H.; Saigusa, H. Dynamics of Excimer Formation and Relaxation in the T-Shaped Benzene Dimer *J. Phys. Chem. A* **1999**, 103, 1014– 1024 DOI: 10.1021/jp983814z

Saigusa, H.; Itoh, M. Dimer Excimer Transformation of Fluorene in a Supersonic Expansion *J. Phys. Chem.***1985**, 89, 5486– 5488 DOI: 10.1021/j100271a034

Ito, M.; Morita, Y.; Saigusa, H. Transformation of Vanderwaals Complexes to Excimer and Exciplex in Jet-Cooled Fluorene and 9-Ethylfluorene *J. Phys. Chem.* **1988**, 92, 5693– 5696 DOI: 10.1021/j100331a029

Saigusa, H.; Lim, E. C. Pump Probe Fluorescence Studies of Excimer Formation and Dissociation for the Vanderwaals Dimer of Fluorene *J. Phys. Chem.* **1991**, 95, 2364– 2370 DOI: 10.1021/j100159a046

Saigusa, H.; Lim, E. C. Localized and Delocalized Excited-States of the Fluorene Dimers *J. Phys. Chem.***1991**, 95, 1194– 1200 DOI: 10.1021/j100156a030

Ichinose, N.; Nishimura, Y.; Yamazaki, I. Excitation-Energy Relaxation and Dimer Formation of Fluorene in Langmuir-Blodgett Monolayer Films *Chem. Phys. Lett.* **1992**, 197, 364– 368 DOI: 10.1016/0009-2614(92)85786-A

Sun, S.; Saigusa, H.; Lim, E. C. Observation of a near-IR Absorption-Band of the Fluorene Excimer by Photodissociation Spectroscopy *J. Phys. Chem.* **1993**, 97, 11635– 11638 DOI: 10.1021/j100147a013

Saigusa, H.; Lim, E. C. Picosecond Photodissociation Study of the Excimer Formation in Van Der Waals Dimers of Aromatic Molecules *Chem. Phys. Lett.* **2001**, 336, 65– 70 DOI: 10.1016/S0009-2614(01)00108-7

Rathore, R.; Abdelwahed, S. H.; Guzei, I. A. Synthesis, Structure, and Evaluation of the Effect of Multiple Stacking on the Electron-Donor Properties of π-Stacked Polyfluorenes *J. Am. Chem. Soc.* **2003**, 125, 8712–8713 DOI: 10.1021/ja035518s

Rathore, R.; Chebny, V. J.; Abdelwahed, S. H. A Versatile and Conformationally Adaptable Fluorene-Based Receptor for Efficient Binding of Silver Cation *J. Am. Chem. Soc.* **2005**, 127, 8012– 8013 DOI: 10.1021/ja051935o

Rathore, R.; Abdelwahed, S. H.; Kiesewetter, M. K.; Reiter, R. C.; Stevenson, C. D. Intramolecular Electron Transfer in Cofacially π-Stacked Fluorenes: Evidence of Tunneling *J. Phys. Chem. B* **2006**, 110, 1536–1540 DOI: 10.1021/jp052737m

Chebny, V. J.; Rathore, R. Convergent Synthesis of Alternating Fluorene-P-Xylene Oligomers and Delineation of the (Silver) Cation-Induced Folding *J. Am. Chem. Soc.* **2007**, 129, 8458– 8465 DOI: 10.1021/ja0687522

Vura-Weis, J.; Abdelwahed, S. H.; Shukla, R.; Rathore, R.; Ratner, M. A.; Wasielewski, M. R. Crossover from Single-Step Tunneling to Multistep Hopping for Molecular Triplet Energy Transfer *Science* **2010**, 328,1547– 1550 DOI: 10.1126/science.1189354

Reilly, N.; Ivanov, M.; Uhler, B.; Talipov, M.; Rathore, R.; Reid, S. A. First Experimental Evidence for the Diverse Requirements of Excimer Vs Hole Stabilization in π-Stacked Assemblies *J. Phys. Chem. Lett.* **2016**,7, 3042– 3045 DOI: 10.1021/acs.jpclett.6b01201

Dietz, T. G.; Duncan, M. A.; Liverman, M. G.; Smalley, R. E. Resonance Enhanced 2-Photon Ionization Studies in a Supersonic Molecular-Beam - Bromobenzene and Iodobenzene *J. Chem. Phys.* **1980**, 73,4816– 4821 DOI: 10.1063/1.440000

Frisch, M. J.; Trucks, G. W.; Schlegel, H. B.; Scuseria, G. E.; Robb, M. A.; Cheeseman, J. R.; Scalmani, G.;Barone, V.; Mennucci, B.; Petersson, G. A.; *Gaussian 09*, Revision E.1; Gaussian, Inc.: Wallingford, CT, **2009**.

Perdew, J. P.; Ernzerhof, M.; Burke, K. Rationale for Mixing Exact Exchange with Density Functional Approximations *J. Chem. Phys.* **1996**, 105, 9982– 9985 DOI: 10.1063/1.472933

Adamo, C.; Barone, V. Accurate Excitation Energies from Time-Dependent Density Functional Theory: Assessing the Pbe0Model for Organic Free Radicals *Chem. Phys. Lett.* **1999**, 314, 152– 157 DOI: 10.1016/S0009-2614(99)01113-6

Grimme, S.; Antony, J.; Ehrlich, S.; Krieg, H. A Consistent and Accurate Ab Initio Parametrization of Density Functional Dispersion Correction (Dft-D) for the 94 Elements H-Pu *J. Chem. Phys.* **2010**, 132, 154104 DOI: 10.1063/1.3382344

Weigend, F. Accurate Coulomb-Fitting Basis Sets for H to Rn *Phys. Chem. Chem. Phys.* **2006**, 8, 1057–1065 DOI: 10.1039/b515623h

Weigend, F.; Ahlrichs, R. Balanced Basis Sets of Split Valence, Triple Zeta Valence and Quadruple Zeta Valence Quality for H to Rn: Design and Assessment of Accuracy *Phys. Chem. Chem. Phys.* **2005**, 7, 3297–3305 DOI: 10.1039/b508541a

Talipov, M. R.; Boddeda, A.; Timerghazin, Q. K.; Rathore, R. Key Role of End-Capping Groups in Optoelectronic Properties of Poly-P-Phenylene Cation Radicals *J. Phys. Chem. C* **2014**, 118, 21400– 21408DOI: 10.1021/jp5082752

Renz, M.; Theilacker, K.; Lambert, C.; Kaupp, M. A Reliable Quantum-Chemical Protocol for the Characterization of Organic Mixed-Valence Compounds *J. Am. Chem. Soc.* **2009**, 131, 16292– 16302 DOI: 10.1021/ja9070859

Renz, M.; Kess, M.; Diedenhofen, M.; Klamt, A.; Kaupp, M. Reliable Quantum Chemical Prediction of the Localized/Delocalized Character of Organic Mixed-Valence Radical Anions. From Continuum Solvent Models to Direct-Cosmo-Rs *J. Chem. Theory Comput.* **2012**, 8, 4189– 4203 DOI: 10.1021/ct300545x

Wessel, J.; Beck, S.; Highstrete, C. Excitonic Interaction in the Fluorene Dimer *J. Chem. Phys.* **1994**, 101,10292– 10302 DOI: 10.1063/1.467909

Meot-Ner, M. Dimer Cations of Polycyclic Aromatics. Experimental Bonding Energies and Resonance Stabillzation *J. Phys. Chem.* **1980**, 84, 2716– 2723 DOI: 10.1021/j100458a011

Horrocks, D. L.; Brown, W. G. Solution Fluorescence Spectrum of Highly Purified Fluorene *Chem. Phys. Lett.* **1970**, 5, 117– 119 DOI: 10.1016/0009-2614(70)80018-5

Ottiger, P.; Koppel, H.; Leutwyler, S. Excitonic Splittings in Molecular Dimers: Why Static Ab Initio Calculations Cannot Match Them *Chem. Sci.* **2015**, 6, 6059– 6068 DOI: 10.1039/C5SC02546J

Rathore, R.; Lindeman, S. V.; Kochi, J. K. Charge-Transfer Probes for Molecular Recognition Via Steric Hindrance in Donor-Acceptor Pairs *J. Am. Chem. Soc.* **1997**, 119, 9393– 9404 DOI: 10.1021/ja9720319